Carbohydrate Polymers 108 (2014) 103–111

Contents lists available at ScienceDirect

Carbohydrate Polymers

journal homepage: www.elsevier.com/locate/carbpol

# Preparation, characterization, mechanical and barrier properties investigation of chitosan–clay nanocomposites

Aris Giannakas[a], Kalouda Grigoriadi[b], Areti Leontiou[a], Nektaria-Marianthi Barkoula[b], Athanasios Ladavos[a,*]

[a] Department of Business Administration of Food and Agricultural Enterprises, University of Patras, Agrinio 30100, Greece
[b] Department of Materials Engineering, University of Ioannina, Ioannina 45110, Greece

ARTICLE INFO

*Article history:*
Received 20 December 2013
Received in revised form 7 March 2014
Accepted 10 March 2014
Available online 19 March 2014

*Keywords:*
Chitosan
Clay
Nanocomposites
Mechanical properties
Barrier properties

ABSTRACT

In the current study the effect of dilution of chitosan acetate solution and of the use of a reflux-solution method on the morphology, the mechanical and water barrier properties of chitosan based nanocomposites is being investigated. Two series of nanocomposite films from two chitosan acetate solutions with 2 w/v% and 1 w/v% in chitosan were prepared, with 3, 5 and 10 wt% Na-montmorillonite (NaMMT) and/or 30 wt% glycerol. Intercalation of NaMMT was more effective in films based on 2 w/v% solutions which presented decreased hydrated crystallinity. Upon NaMMT addition an enhancement was found in stiffness and strength (up to 100%) and a remarkable decrease in the elongation at break (up to 75%) and water vapor permeability (WVP) (up to 65%). This enhancement was less pronounced in 1 w/v% systems. Addition of glycerol had a negative effect on the stiffness, strength and WVP, and a positive effect on the elongation at break and the absorbed water. Compared with the conventional solution cast method, the reflux treatment led to a significant improvement of the tested properties of nanocomposite films.



## 1. Introduction

Environmental concerns caused by the solid waste after use of petrochemical-based plastic packaging materials have increased the interest in biodegradable packaging materials (Han & Gennadios, 2005). These materials are often formulated with natural biopolymers, such as polysaccharides, proteins, and natural gums, capable of forming a cohesive and continuous matrix (Cuq, Gontard, & Guilbert, 1998; Han & Gennadios, 2005).

Chitosan, the cationic (1-4)-2-amino-2-deoxy-β-D-glucan, is industrially produced in various quality grades from chitin, the second most abundant polysaccharide in nature (Muzzarelli, 2012; Muzzarelli et al., 2012) and has been studied extensively for applications in the packaging industry (Rhim & Ng, 2007) owing to its biodegradability, biocompatibility, and absence of toxicity. However, it's mechanical and water barrier properties should be improved.

A commonly used approach to enhance mechanical and barrier properties of chitosan to meet standards for a wide range of applications is through the introduction of reinforcement at the nanoscale (Jason, Marroquina, Rheea, & Park 2013; Lavorgna et al., 2014; Muzzarelli & Muzzarelli, 2002; Muzzarelli, 2011). The addition of layered silicates and in particular montmorillonite (MMT) in chitosan has been extensively studied (Günister, Pestreli, Unlu, Atici, & Gungor, 2007; Hong et al., 2011; Oguzlu & Tihminlioglu, 2010; Rhim, Hong, Park, & Ng, 2006; Tang et al., 2009; Wang et al., 2005; Wang, Du, Yang, Tang, & Luo, 2006; Xu, Ren, & Hanna, 2006). It was been shown that both the structure of chitosan/MMT nanocomposites and their thermal stability are strongly affected by the solvent-casting procedure used (Günister et al., 2007). In Ref. Wang et al. (2005) the effect of both acetic acid residue and the hydrogen bonds formed between chitosan and MMT on the nanocomposite properties have investigated. They demonstrated that the residual acetic acid accelerates the thermal decomposition of chitosan and decreases its crystallinity level. The effect of the solution's temperature and acidity (e.g. pH 5, 8 and 12) on the MMT dispersion has been also documented (Potarniche et al., 2012). It was found that for pH 5 and high solution temperatures a higher quantity of chitosan was intercalated between the silicate layers compared to the samples processed at room temperature or at other pHs. From this it can be assumed that at pH 5 the chitosan chains are oriented preferentially between the silicate layers.

* Corresponding author at: Department of Business Administration of Food and Agricultural Enterprises, Laboratory of Food Technology, University of Patras, Agrinio 30100, Greece. Tel.: +30 2641074126; fax: +30 2641091703.
*E-mail addresses:* agiannak@cc.uoi.gr (A. Giannakas), kalouda.grigoriadi@gmail.com (K. Grigoriadi), aleontiu@cc.uoi.gr (A. Leontiou), nbarkoul@cc.uoi.gr (N.-M. Barkoula), alantavo@cc.uoi.gr (A. Ladavos).

http://dx.doi.org/10.1016/j.carbpol.2014.03.019
0144-8617/

**Table 1**
Amounts (g and wt%) of chitosan, glycerol, NaMMT used for the preparation of chitosan, chitosan/glycerol, chitosan/NaMMT and chitosan/glycerol/NaMMT films via the reflux solution method as well as $d_{001}$, Young's modulus ($E$), tensile strength ($\sigma_{uts}$), elongation at break ($\varepsilon_b$), and water vapor permeability (WVP) values.

| Code name | Chitosan (g)-wt% | Glycerol (g)-wt% | NaMMT (g)-wt% | $d_{001}$ (nm) | $E$ (MPa) | $\sigma_{uts}$ (MPa) | $\varepsilon_b$ (%) | WVP (g h$^{-1}$ m$^{-2}$) |
|---|---|---|---|---|---|---|---|---|
| *Chitosan solution 2 w/v% in 1 v/v% acetic acid (HAc)* | | | | | | | | |
| CS_2 | 2–100% | – | – | – | 3411 ± 410 | 123.65 ± 4.55 | 15.65 ± 2.30 | 9.5 ± 0.5 |
| CS3MMT_2 | 2–97% | – | 0.0583–3% | – | 6940 ± 461 | 208.50 ± 4.97 | 6.05 ± 0.53 | 3.3 ± 0.3 |
| CS5MMT_2 | 2–95% | – | 0.0950–5% | 1.66 | 4866 ± 307 | 151.00 ± 9.57 | 5.00 ± 0.85 | 5.0 ± 0.3 |
| CS10MMT_2 | 2–90% | – | 0.1820–10% | 1.74 | 6156 ± 117 | 122.50 ± 15.72 | 3.93 ± 0.83 | 3.2 ± 0.2 |
| CS30G_2 | 2–70% | 0.857–30% | – | | 1403 ± 232 | 118.00 ± 11.90 | 67.55 ± 6.43 | 17.9 ± 0.5 |
| CS30G3MMT_2 | 2–67% | 0.896–30% | 0.0896–3% | – | 416 ± 2 | 78.00 ± 7.48 | 82.90 ± 7.40 | 15.5 ± 0.4 |
| CS30G5MMT_2 | 2–65% | 0.926–30% | 0.1540–5% | 2.09 | 1043 ± 58 | 82.40 ± 12.40 | 61.85 ± 12.15 | 14.9 ± 0.4 |
| CS30G10MMT_2 | 2–60% | 1.004–30% | 0.3370–10% | 2.07 | 608 ± 37 | 92.60 ± 6.12 | 89.25 ± 5.70 | 13.3 ± 0.3 |
| *Chitosan solution 1 w/v% in 0.5 v/v% acetic acid (HAc)* | | | | | | | | |
| CS_1 | 2–100% | – | – | – | 3527 ± 247 | 108.00 ± 6.96 | 15.38 ± 1.70 | 16.2 ± 0.4 |
| CS3MMT_1 | 2–97% | – | 0.0583–3% | 1.69 | 4264 ± 202 | 111.00 ± 2.63 | 5.15 ± 2.18 | 14.1 ± 0.3 |
| CS5MMT_1 | 2–95% | – | 0.0950–5% | 1.81 | 4748 ± 78 | 126.00 ± 11.4 | 9.58 ± 2.38 | 12.7 ± 0.3 |
| CS10MMT_1 | 2–90% | – | 0.1820–10% | 1.83 | 4480 ± 402 | 128.00 ± 8.20 | 6.13 ± 2.38 | 11.9 ± 0.2 |
| CS30G_1 | 2–70% | 0.857–30% | – | – | 1178 ± 125 | 67.25 ± 12.04 | 50.68 ± 9.23 | 23.8 ± 0.4 |
| CS30G3MMT_1 | 2–67% | 0.896–30% | 0.0896–3% | 2.05 | 31 ± 5 | 25.25 ± 3.34 | 56.63 ± 0.80 | 23.6 ± 0.5 |
| CS30G5MMT_1 | 2–65% | 0.926–30% | 0.1540–5% | 2.69 | 96 ± 10 | 58.75 ± 4.20 | 92.18 ± 5.28 | 22.8 ± 0.5 |
| CS30G10MMT_1 | 2–60% | 1.004–30% | 0.3370–10% | 2.03 | 48 ± 8 | 10.47 ± 0.65 | 37.50 ± 4.40 | 20.9 ± 0.5 |

The synergistic effect of plasticizer and layer silicate on the properties of chitosan based films has been reported in Ref. Lavorgna, Piscitelli, Mangiacapra, and Buonocore (2010). It was concluded that there is a competition between local structure and long-range order in self-associated chitosan and chitosan based nanocomposite films, controlled by electrostatic interactions, hydrogen bonding and crystallization processes, which has not been yet fully understood.

Based on the above the aim of the current study is to elaborate on the solution casting method in order to enhance intercalation/exfoliation and thus improve the performance of the NaMMT reinforced chitosan films. Since the temperature, the acidity of the chitosan solution and the amount of acetic acid residues are of key importance for the degree of intercalation, the amount of hydrogen bonding and the crystallinity level of the final films, a reflux-solution methodology has been introduced for the preparation of chitosan based nanocomposites. The reflux condenser does not allow any water or acetic acid to evaporate during processing, and is expected to result in higher mobility and more homogenous charge of the chitosan's amine groups and thus more effective interaction between chitosan and NaMMT. The reflux-solution methodology is applied on two different chitosan acetate dilution levels (2 w/v% and 1 w/v% in chitosan) in order to define the required acetate concentration for effective charge of the chitosan's chains with limited residues. Selected films were prepared with the conventional solution cast method for comparison. Also the effect of the: (i) addition of different amounts of NaMMT varying from 3 wt% to 10 wt% and (ii) addition of both glycerol (in a standard content of 30 wt%) and clay were studied. The obtained morphology as well as the mechanical and barrier properties of the nanocomposite films was investigated.

## 2. Experimental

### 2.1. Materials

Medium molecular weight chitosan with viscosity of 200–800 cP, 1 wt% in 1% acetic acid at 25 °C (Cat. No. 448877) with a deacetylation degree 75–85% was purchased from Sigma–Aldrich. The pristine clay Na-montmorillonite (NaMMT) (Nanomer® PGV – hydrophilic betonite nanoclay) and glacial acetic acid (HAc) was bought from Sigma–Aldrich. Glycerol used as plasticizer was purchased from Carlo Erba.

### 2.2. Preparation of chitosan nanocomposite films

2 w/v% chitosan solution was prepared by dissolving 20 g of chitosan powder in 1000 ml of 1 v/v% aqueous HAc solution, under vigorous stirring for 24 h at 70 °C. Then the mixture (pH ≈ 4.4) was left to cool down at room temperature. 500 ml of the as above prepared chitosan solution was diluted in 500 ml distilled water to make a second chitosan solution with concentration of 1 w/v% (pH ≈ 4.7). The two chitosan solutions were stored for further use.

(i) 100 ml of 2 w/v% and (ii) 200 ml of 1 w/v% chitosan solution were respectively mixed with the appropriate amounts of NaMMT and glycerol in order to reach a final clay concentration of 3, 5 and 10 wt% and glycerol concentration of 30 wt%. The amounts of chitosan, clay and plasticizer used for each sample are listed in Table 1. The chitosan–clay and chitosan–glycerol–clay mixtures were refluxed for 1 h, spread onto plastic dishes (14 cm diameter), dried at ambient conditions (≈22 °C) for 5 days and finally the plastic films were peeled off.

### 2.3. XRD analysis

The X-ray diffraction analysis of the obtained films was performed on a D8 Advanced Brüker diffractometer with $CuK_a$ radiation ($\lambda$ = 1.5418 Å) and the d-spacing of the clay containing samples was estimated from the 0 0 1 reflection.

### 2.4. Tensile measurements

Tensile tests were performed according to ASTM D882 using a miniature material tester with a 1000 N load cell. Three to five samples of each formulation were clamped between the grips (30 mm initial distance) and tensioned at a crosshead speed of 10 mm/min. The shape of the samples was dumbbell with gauge dimensions of 15 mm × 3 mm × 0.22 mm. Force (N) and deformation (mm) where recorded during the test. The results obtained from the mini-tester can only be used for comparison, because the strain values are based on the rotational movement of the drive shaft. Baseline samples (not containing nanoclay or glycerol) were tested at the beginning of each set of samples for comparison.

### 2.5. Water sorption

Selected films were cut in small pieces (12 mm × 12 mm), desiccated overnight under vacuum and weighed to determine their

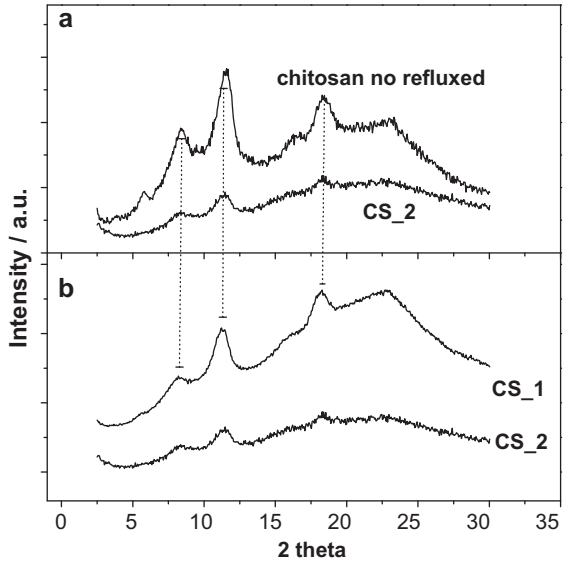


**Fig. 1.** XRD patterns of: (a) 2 w/v% chitosan film no refluxed in comparison with 2 w/v% chitosan refluxed film (CS_2) and (b) 2 w/v% chitosan refluxed film (CS_2) in comparison with 1 w/v% chitosan refluxed film (CS_1).

dry mass. The weighed films were placed in closed beakers containing 30 ml of water (pH = 7) and stored at $T = 25\,^{\circ}C$. The sorption plots were evaluated by periodical weighting of the samples until equilibrium was reached. The water gain (W.G.) was calculated as follows:

$$\text{W.G. } (\%) = (m_{\text{Wet}} - m_{\text{Dry}})/m_{\text{Dry}} \times 100 \quad (1)$$

where $m_{\text{Wet}}$ and $m_{\text{Dry}}$ are the weight of the wet and dry film, respectively.

### 2.6. Water vapor permeability (WVP)

Water vapor permeability (WVP) of the prepared films was determined at 38 °C using the apparatus and methodology described in the ASTM E96/E 96M-05 and in our previous publication (Giannakas, Spanos, Kourkoumelis, Vaimakis, & Ladavos, 2008). Films with 0.10 mm thickness were sealed by a rubber O-ring on top of Plexiglas test bottles containing dried silica gel and then placed in a glass desiccator with 200 ml saturated magnesium nitrate solution (50% relative humidity (RH)). Test bottles were weighed periodically for 24 h and the WVP was calculated according to the following equation:

$$\text{WVP} = \left(\frac{G}{t}\right)/A \quad (2)$$

where $G$ is the weight gain of the tested bottles in $g$, $t$ is the time in hours, $G/t$ is the slope of the straight line in the diagram $G = f(t)$ and $A$ is the permeation area.

## 3. Results and discussion

### 3.1. XRD analysis

XRD patterns of chitosan and chitosan based nanocomposite films in the range of 2–30° are shown in Figs. 1 and 2. The d-spacing values for composites containing NaMMT are listed in Table 1. In Fig 1a and b the effects of dilution (CS_2 vs. CS_1) and/or use of reflux process (CS_2 vs. CS_2-no reflux) on the XRD patterns of chitosan films are presented.

Characteristic peaks of chitosan at around $2\theta = 8°$, 11°, 18° and 23° are shown in agreement with previous publications (Lavorgna et al., 2010; Rhim, Hong, Park, & Ng, 2006; Tang et al., 2009; Wang et al., 2005). The two former peaks indicate a hydrated crystallite structure due to the integration of water molecules in the crystal lattice. The peak at 18° is attributed to the regular crystal lattice of chitosan (Kittur, Kumar, & Tharanathan, 2003) whereas the broaden peak around 23° indicates an amorphous structure of chitosan (Lavorgna et al., 2010; Rhim et al., 2006; Tang et al., 2009; Wang et al., 2005). The crystallinity of chitosan is strongly depended on its treatment such as dissolving, precipitation and drying, as well as its origin and characteristics, such as degree of deacetylation and molecular weight (Jaworska, Sakurai, Gaudon, & Guibal, 2003; Rhim et al., 2006). Reflux treatment affects the crystallinity degree of chitosan which is depicted by the significant decrease of the characteristic peaks intensity at 8°, 11° and 18° of the CS_2 sample as is shown in Fig. 1a. The dilution of 2 w/v% chitosan solution to 1 w/v% causes an increment in the intensities of characteristic peaks at 8°, 11° and 18° as it shown in Fig. 1b.These results can be explained on the following basis: Higher peaks with sharper reflections indicate improved crystallinity or denser packing in the main chain and better organized long range structure. Films cast from chitosan/HAc solutions contain charged and neutral amine groups (Thakhiew, Devahastin, & Soponronnarit, 2010). Because of the higher pH value of diluted chitosan acetate solution (pH = 4.7) in comparison with initial chitosan acetate solution with pH = 4.4 a lower fraction of amine groups is expected to be protonated in the CS_1 samples compared to the CS_2 samples. The presence of higher amount of charged groups, which introduce strong electrostatic interactions between the $-NH_2$ and $-NH_3^+$ groups, could hinder the packing of the chains following the usual hydrogen bonding pattern (Kittur et al., 2003). As underlined in Ref. Gartner et al. (2011), there is an apparent contradiction in stating that charged films tend toward a much more regular long-range order but that the least charged one is the best organized. It can be rationalized by taking into account that the stronger rigidity may prevent the structure to reorganize, which is needed to accomplish long range order. Next to that the lower acidity in the CS_1 solution might result in lower amounts of HAc residues. As demonstrated in Ref. Wang et al. (2005) films without HAc residues presented higher crystallinity compared to those with HAc residues.

In Fig. 2 the XRD patterns of chitosan/NaMMT (a, b), chitosan/glycerol (c and d) and chitosan/glycerol/NaMMT (e and f) films obtained from 2 w/v% and 1 w/v% solutions are presented.

In Fig. 2a, it is obvious that the addition of NaMMT in 2 w/v% chitosan's solution does not affect the crystallinity of the obtained samples while in the case of films obtained from 1 w/v% solution (Fig. 2b), the clay addition causes a decrease in the crystallinity of chitosan. The XRD pattern of NaMMT clay (dashed line) presents a distinctive diffraction peak at 7.3° which corresponds to a $d_{001}$ spacing of 1.2 nm. The absence of XRD reflection, characteristic of the clay peak, for films prepared from 2 w/v% solution and 3 wt% clay addition (Fig. 2a) is indicative of exfoliated or partially exfoliated structure. In the case of 5 and 10 wt% NaMMT addition (CS5MMT_2 and CS10MMT_2) very low, clay related, XRD peaks are present, but shifted to lower $2\theta$ angles (i.e., higher d-spacing values). The basal spacing values for the composites with 5 and 10 wt% NaMMT loadings were estimated 1.66 and 1.77 nm, respectively. This is indicative of an intercalated structure where the polymer chains are incorporated between the silicate layers, increasing their gallery height but maintaining their layered stacking with alternating polymer silicate layers. Similar XRD patterns with 2 w/v% chitosan acetate solution samples were observed for samples prepared from diluted 1 w/v% chitosan acetate solution (Fig. 2b) with $d_{001}$ spacing values ranging between 1.69 and 1.83 nm. The results reported here are in line with previous publications. In Ref. Lavorgna et al. (2010) it was concluded that in the case of chitosan/clay films, without glycerol addition, it is

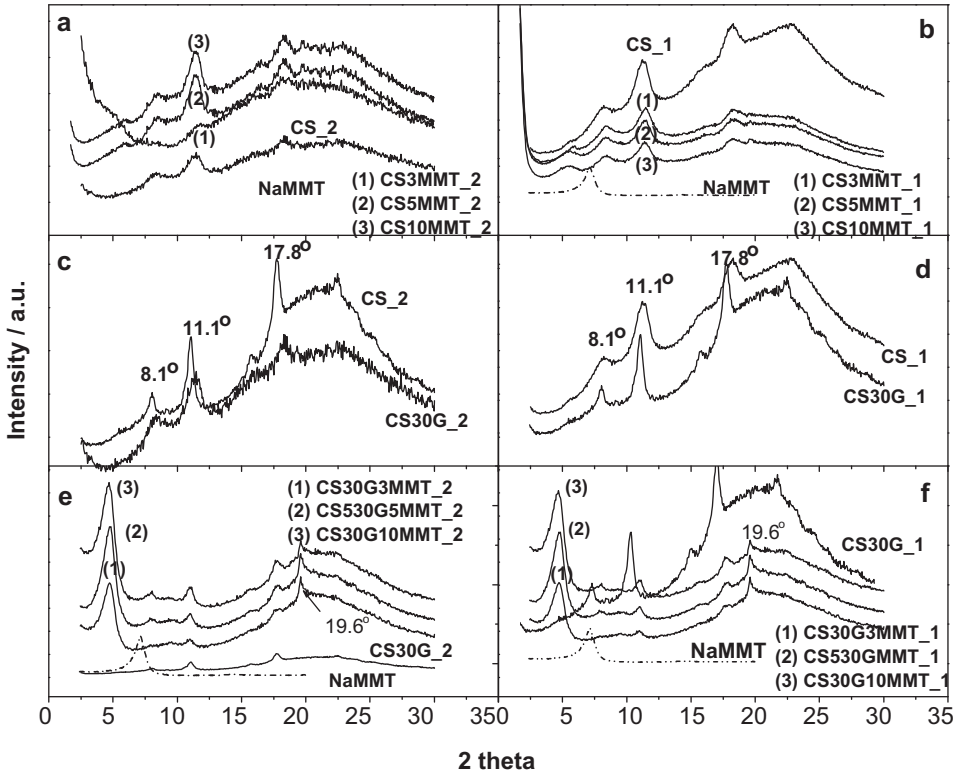


**Fig. 2.** XRD patterns of: (a) and (b) chitosan/NaMMT; (c) and (d) chitosan/glycerol and (e) and (f) chitosan/glycerol/NaMMT films. On the left hand part, graphs (a, c and e): XRD patterns for films prepared with chitosan solution 2 w/v%. On the right hand part, graphs (b, d and f): XRD patterns for films prepared with chitosan solution 1 w/v%. The XRD patterns of chitosan and NaMMT have been included in (a), (b), (e), (f) graphs for comparison.

possible to detect a broad shoulder, in the range of $2\theta$ of 5–7°, generally attributed to poor or monolayer intercalation of chitosan macromolecules into the NaMMT stacks. Chitosan/NaMMT nanocomposite films with a significant intercalated structure have been prepared as a result of the good compatibility of chitosan with NaMMT (Rhim et al., 2006). This compatibility was caused mainly by the ion exchange between $Na^+$ ions of the NaMMT and the positive charged amine groups of chitosan.

In Fig. 2c and d the XRD patterns of chitosan/glycerol films obtained from 2 w/v% and 1 w/v% solution are shown. The addition of glycerol results in a pronounced peak at 17.8°. Because of the hydrophilic and polycationic nature of chitosan in acidic media, this biopolymer has good miscibility which is attributed to the interaction of glycerol molecules with chitosan macromolecules (Ziani, Oses, Coma, & Mate 2008). Glycerol favors the chains mobility and thus the chitosan crystallization process in the early stage of the post-processing aging (Epure, Griffon, Pollet, & Avérous, 2011). In Ref. Ziani et al. (2008) the effect of glycerol addition on two different types of chitosan with deacetylation degree of 96% and 60% has been studied and in both cases chitosan's crystallinity was improved.

In Fig. 2e and f the XRD patterns of chitosan/glycerol/NaMMT films obtained from 2 w/v% and 1 w/v% chitosan solution are shown. The combined addition of glycerol and clays resulted in great enhancement of the chitosan crystallinity of the nanocomposite films prepared with 2 w/v% chitosan solution. This indicates that the presence of clay facilitates the distribution of glycerol within the chitosan matrix and the interaction of glycerol molecules with chitosan macromolecules (Ziani et al., 2008). The combined addition of glycerol and clay had an opposite effect in films obtained from low content chitosan solution leading to a decrease of the XRD-peaks intensities. It is assumed that in films obtained from low content chitosan's solution, chitosan macromolecules are less charged leading to weaker electrostatic/ion exchange and hydrogen bond interactions between chitosan, NaMMT, water and glycerol. In addition a new peak at $2\theta \approx 19.6°$ appeared in XRD patterns of all obtained films. This diffraction peak is characteristic (Bangyekan, Aht-Ong, & Srikulkit, 2006; Ziani et al., 2008) for chitosan films prepared using acetic acid solution as solvent.

XRD patterns of all chitosan/glycerol/NaMMT films present intense reflection peaks at low angle area of 3.7–4.7°. These peaks correspond to the clay basal spacing and provide a strong evidence of intercalated structure where the polymer plus glycerol chains are incorporated between the silicate layers. The addition of glycerol favors the opening of the clay galleries resulting in intercalated nanocomposites with higher d-space in comparison to samples without glycerol. As previously reported (Darder, Colilla, & Ruiz-Hitzky, 2003), the thickness of the individual sheet of chitosan chain is 0.38 nm. In this case, the diffractograms support the intercalation of chitosan as mono and/or bilayer. In Ref. Lavorgna et al. (2010) has been reported that the addition of glycerol reduces the extent of hydrogen-bonding interactions between chitosan and clay sheets' edges by favoring preferential interactions between glycerol molecules and clay. This hinders the flocculation process and facilitates the intercalation, where NaMMT sheets stack orientated in the film.

On the basis of XRD patterns, it can be stated that crystallinity of chitosan decreased with the reflux process while the dilution of initial chitosan solution from 2 w/v% to 1 w/v% and the addition of glycerol favors the crystallinity of the obtained chitosan based samples.

### 3.2. Tensile measurements of chitosan, chitosan/glycerol, chitosan/NaMMT and chitosan/glycerol/NaMMT films

The stress–strain curves of the tested specimens are being presented in Figs. 3 and 4, while the average values along with the standard deviation of the Young's modulus ($E$), tensile strength ($\sigma_{uts}$) and elongation at break ($\varepsilon_b$) of the films prepared via the reflux solution method are provided in Table 1.

More specifically, Fig. 3a and b illustrates the effect of the dilution degree (2 w/v% vs. 1 w/v% chitosan solution) on the stress–strain behavior of the chitosan and chitosan/glycerol films, respectively. As seen in Fig. 3a the dilution degree has a clear effect on the yield and tensile strength, with the CS_2 films presenting app. 15% higher values compared to CS_1 films. Almost identical values are being obtained in terms of Young's Modulus and elongation at break (see Table 1). The higher strength obtained in the case of the CS_2 films can be attributed to more efficient stress transfer between the adjacent chains due to the strong electrostatic interactions between the $-NH_2$ and $-NH_3^+$ groups. The effect of the dilution after the addition of plasticizer is being depicted in Fig. 3b. Although curves 3 and 4 are qualitatively similar, there is a pronounced difference in all quantitative parameters, like stiffness, yield and tensile strength, and elongation at break. The CS30G_2 specimens present almost two times higher strength (at yield and break) and elongation at break compared to those with 1 w/v% HAc. Due to the lower acidity of the diluted films a weaker hydrogen bond network was established between the amino groups and the glycerol chains. On the other hand the extensive deformation strengthening in undiluted systems (CS30G_2) suggests the creation of a long-range order and the formation of hydrogen bonding (Petrova et al., 2012) after the addition of glycerol. This is in line with previous observations, where FTIR results confirmed that glycerol molecules displace HAc in the formation of hydrogen bonding with amine groups (Lavorgna et al., 2010).

The effect of NaMMT addition on the tensile response of the chitosan and chitosan/glycerol films is being depicted in Fig. 4a–d for the two different chitosan solutions used (2 w/v% vs. 1 w/v%).

In Fig. 4a the stress–strain curves of NaMMT composite films prepared from the 2 w/v% chitosan solution is being presented. The addition of NaMMT results in a pronounced enhancement of the stiffness (up to 100%) and strength (up to 70%) and a dramatic decrease in the elongation at break (up to 75%) of all clay-added systems. The CS3MMT_2 system is the one with the highest stiffness (app. 7 GPa), strength (app. 210 MPa) and elongation at break (app. 6%) among all CS_2 NaMMT modified composites. This is in agreement with the XRD results, which indicated that at 3 wt% NaMMT an exfoliated nanocomposite was obtained. Further addition of NaMMT leads in intercalated structures which limited the polymer–clay interactions and thus their reinforcing ability.

In Fig. 4b the effect of NaMMT addition is being illustrated for the diluted systems (CS_1 nanocomposites). The ductile response of the CS_1 films is maintained after the addition of NaMMT with a smaller enhancement in stiffness (up to 35%) and strength (up to 18%) and a relative lower decrease in the elongation at break (up to 65%) compared to the respective CS_2 films. The systems with 3 wt% NaMMT presented the lowest enhancement in all mechanical properties. This is in agreement with the XRD results, since this system had the lowest d-space value.

Fig. 4c presents the combined effect of glycerol and NaMMT on the tensile response of the CS_2 based nanocomposites. The first observation is that the addition of NaMMT results in a direct reduction of the stiffness and the strength of the chitosan/glycerol and in most cases in an increase in the elongation at break. The XRD results indicated that an intercalated structure is being obtained after the addition of NaMMT in the chitosan/glycerol matrix. Based on that one would expect that the nanocomposite systems would present an enhancement in strength and stiffness, however this is not the case. Although these results are somewhat peculiar, similar trends have been documented in Ref. Xie et al. (2013) when studying the dynamic mechanical properties of chitosan/glycerol/NaMMT composites. They have found that the addition of 2.5 wt% NaMMT led to a reduction of the relaxation temperatures of the nanocomposites, which was associated with the more homogenous distribution of water and glycerol across the system, resulting in better plasticization effect (Xie et al., 2013). On the addition of 5 wt% NaMMT higher relaxation temperatures were found, indicative of an extra restriction on the movement of the chitosan chains (Xie et al., 2013).

A completely different stress–stain behavior is being obtained after the addition of NaMMT in diluted chitosan/glycerol systems (Fig. 4d). The CS_1/glycerol based nanocomposites behave like hyperelastic materials rather than like ductile polymers. They are very extensible at low strain but resist some deformation at higher strain especially with the addition of 5 wt% NaMMT. It seems that due to the low concentration of HAc there is very limited amount of electrostatic interactions between the NaMMT and chitosan. It is assumed that more water and glycerol are distributed within the chitosan network, inducing a very obvious plasticization effect. The extend of hydrated chitosan crystals was confirmed from the intensities of the XRD patterns, where chitosan crystalline peaks are double as high in the case of the chitosan/glycerol/MMT_1 than in chitosan/glycerol/MMT_2 films.

Fig. 5 illustrates the effect of the reflux process on the mechanical properties of CS_2 and CS_1 based nanocomposite films without glycerol. It is very interesting to note that although the mechanical properties of the unreinforced chitosan are comparable before and after the application of the reflux processing, reflux resulted in a fourfold increase of the stiffness and strength of the nanocomposite films, as seen in Figs. 5a and b while elongation at break presented a respective decrease (Fig. 5c). Next to that, after the application of the reflux process the same order is followed in all mechanical properties as a function of the NaMMT content. Finally, very little deviation is being observed in the elongation data after application of reflux (Fig. 5c). The reflux condenser does not allow any water or acetic acid to evaporate during processing, resulting in homogenous films with more effective interaction between the different constituents of the nanocomposite films. Overall very different values can be found in the open literature for chitosan, chitosan/glycerol and their NaMMT nanocomposites (Hong et al., 2011; Lavorgna et al., 2010; Petrova et al., 2012; Suyatma, Tighzert, Copinet, & Coma, 2005; Thakhiew et al., 2010; Wang et al., 2005; Xie et al., 2013). The stiffness and strength results obtained here after applying the reflux process are comparable with those in Ref. (Petrova et al., 2012) and higher than those found in most publications stating stiffness of app. 3.5–5 GPa, strength of app. 30–60 MPa after the addition of clay in chitosan matrices (Hong et al., 2011; Lavorgna et al., 2010; Wang et al., 2005). The observed enhancement of the properties of the nanocomposite films tested here can be attributed to the novel reflux-solution process used for the preparation of chitosan/NaMMT and chitosan/glycerol/NaMMT films.

### 3.3. Water sorption

Fig. 6a and b illustrates the effect of the dilution degree (2 w/v% vs. 1 w/v% chitosan solution) and NaMMT addition on the water sorption profiles for films not containing glycerol. CS_2 and

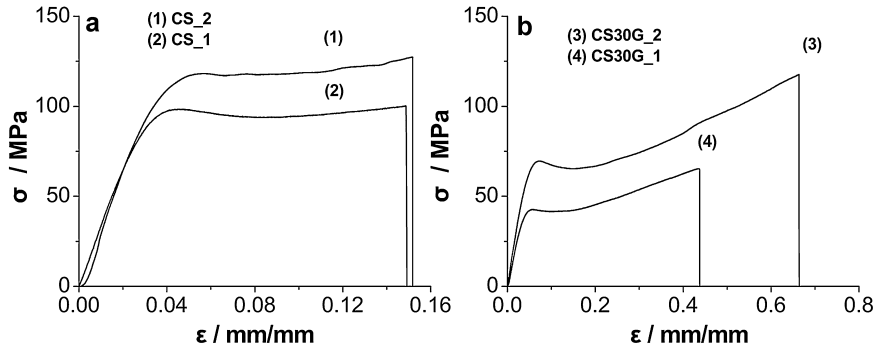


**Fig. 3.** Stress–strain curves of: (a) chitosan films and (b) chitosan/glycerol films prepared via the reflux solution method with 1 w/v% (curves: 2, 4) and 2 w/v% (curves: 1, 3) chitosan solution.

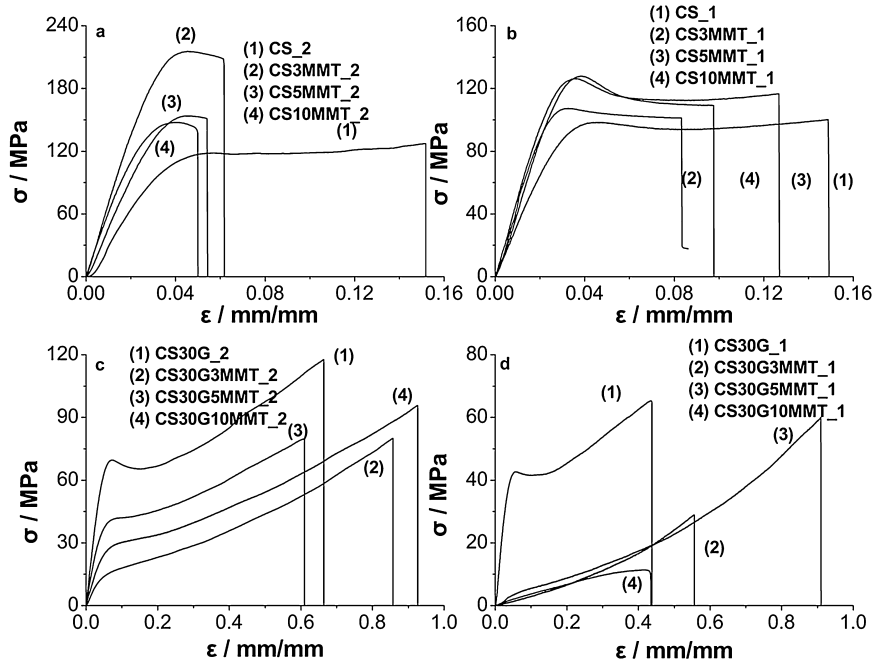


**Fig. 4.** Stress–strain curves of: (a) chitosan/NaMMT, (b) chitosan/NaMMT, (c) chitosan/glycerol/NaMMT and (d) chitosan/glycerol/NaMMT films. On the left hand part, graphs (a and c): films prepared with chitosan solution 2 w/v%. On the right hand part, graphs (b and d): films prepared with chitosan solution 1 w/v%. The response of chitosan and chitosan/glycerol has been included in (a), (b) and (c), (d) graphs, respectively for comparison.

CS5MMT_2 films have been also prepared via the conventional solution cast method (designated as no reflux in the graph) and added in Fig. 6a.

The data show that chitosan and chitosan/NaMMT composite films rapidly absorb large amounts of water and most tested films without glycerol dissolve within 120 min of exposure. The addition of NaMMT results in a considerable reduction of the absorbed water in both undiluted and diluted nanocomposites up to 60% and 75%, respectively. The decrease of absorbed water with the addition of NaMMT was previously reported in Ref. Rhim et al. (2006). Comparing Fig. 6a and b it is obvious that the dilution of the chitosan acetate solution results in considerable reduction of the absorbed

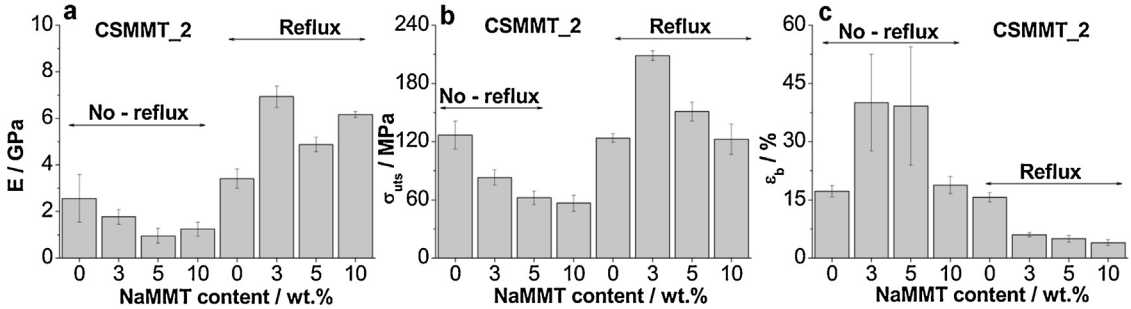


**Fig. 5.** Effect of the reflux processing on: (a) Young's-modulus, (b) tensile strength and (c) elongation at break of chitosan/NaMMT films with various NaMMT contents (chitosan solution 2 w/v%).

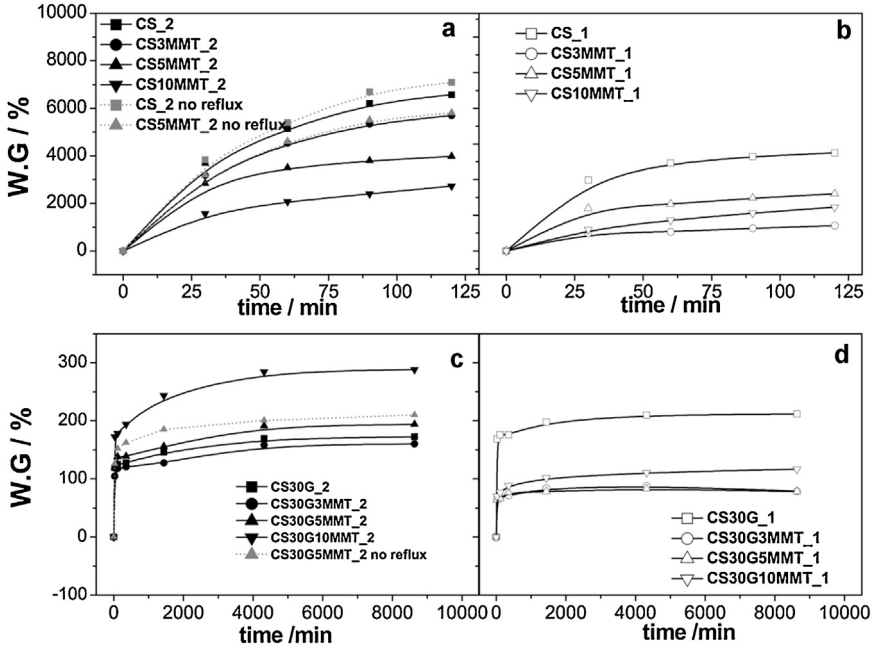


**Fig. 6.** Water sorption profiles at 25 °C and pH = 7 of films obtained: (a) chitosan/NaMMT films, (b) chitosan/NaMMT, (c) chitosan/glycerol/NaMMT and (d) chitosan/glycerol/NaMMT films. On the left hand part, graphs (a and c): films prepared with chitosan solution 2 w/v%. On the right hand part, graphs (b and d): films prepared with chitosan solution 1 w/v%. The response of chitosan and chitosan/glycerol has been included in (a), (b) and (c), (d) graphs, respectively for comparison.

water. This can be attributed to HAc residues in the case of CS_2 based nanocomposites, which facilitate swelling of chitosan. Finally the use of the reflux method did not drastically alter the response of the unreinforced CS but resulted in a considerable reduction (app. 30%) of the absorbed water in the case of the CS5MMT_2 systems. This implies that the water reduction is due to the more efficient intercalation of NaMMT after reflux.

Fig. 6c and d illustrates the effect of the dilution degree (2 w/v% vs. 1 w/v% chitosan solution) and NaMMT addition on the water sorption profiles for films containing glycerol. Water sorption curves reach equilibrium and the amount of absorbed water is one order of magnitude lower in comparison to that for films without glycerol. Thus, the presence of glycerol gives a higher stability to the samples. Similar effects on the water sorption behavior of glycerol added chitosan/NaMMT system have been reported in Ref. Lavorgna et al. (2010). Dilution and use of the reflux methodology resulted in similar trends in films containing glycerol as those seen in Fig. 6a and b. It is interesting to note that the NaMMT addition was beneficial in the case of diluted nanocomposites, while in CS30G_2 films the addition of NaMMT deteriorated the water absorption profiles. Based on the stress–strain response of CS30G_1 nanocomposites, it has been assumed that due to the limited electrostatic interactions NaMMT facilitated the distribution of water and glycerol within the chitosan network, inducing a very obvious plasticization effect.

### 3.4. Water vapor permeability

In Fig. 7a and b representative plots of the weight gain of the test bottles as a function of time are shown during WVP experiments for neat chitosan films (CS_2, CS_1), chitosan with 5 wt% NaMMT films (CS5MMT_2, CS5MMT_1) and chitosan films with 30 wt% glycerol and 5 wt% NaMMT (CS30G5MMT_2, CS30G5MMT_1). Fig. 7a illustrates the effect of dilution while Fig. 7b the effect of the use of the reflux methodology on the WVP response of the selected films. It is obvious from the obtained results that dilution leads to an obvious increase in the WVP and the same holds for films prepared via the conventional solution method (no reflux). The higher WVP of all films prepared by diluted 1 w/v% chitosan solution as well as no-reflux films in comparison to films obtained by 2 w/v% chitosan solution could be ascribed to the higher hydrated crystallinity of the respective films as shown in Fig. 1.

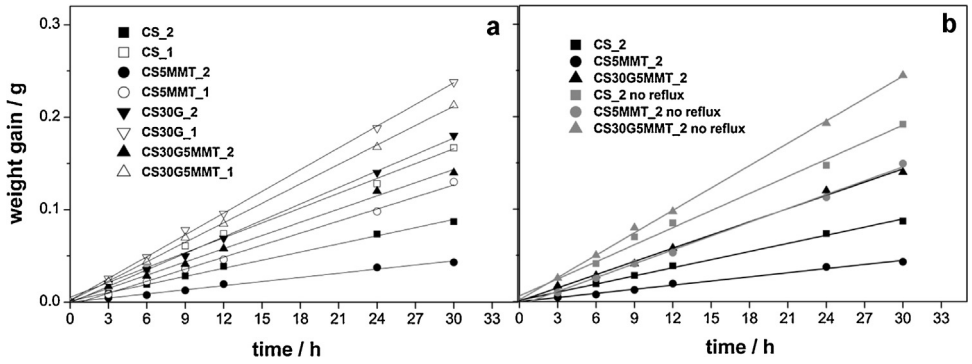


**Fig. 7.** Weight gain of the WVP's bottles (due to water uptake of the absorbant) as a function of time for selected chitosan based films: (a) effect of dilution and (b) effect of the preparation methodology (reflux vs. no reflux).

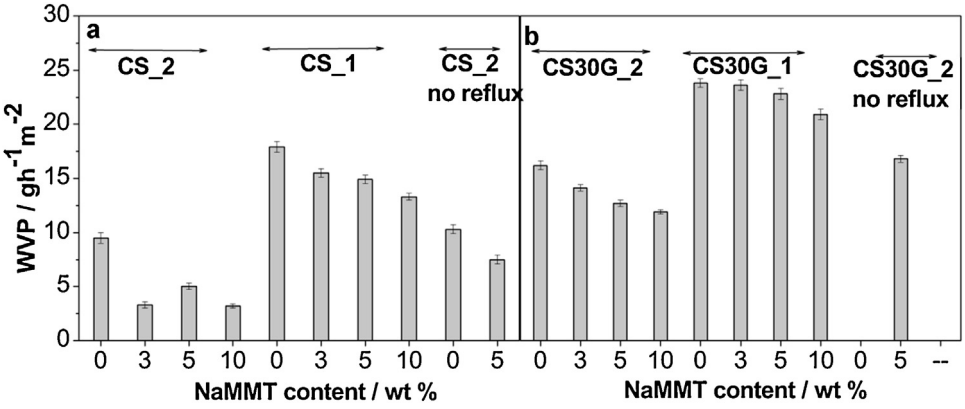


**Fig. 8.** WVP values as a function of NaMMT content, dilution and preparation methodology (reflux vs. no reflux) for (a) chitosan and (b) chitosan/glycerol based films.

Since the relationship between the weight gain and time for all tested samples is linear, Eq. (2) has been applied for the calculation of the water vapor permeability (WVP) data which are listed in Table 1 for the films prepared via the reflux solution method. For direct comparison the WVP data are plotted in Fig. 8a and b for films without and with glycerol. WVP values from selected no-reflux films have been also calculated and added in Fig. 8.

The lowest WVP values are found for films obtained from 2 w/v% chitosan solution and their nanocomposites. Dilution (as discussed above) results in a twofold increase in the WVP values for tested chitosan based films. The same effect is being observed with the addition of glycerol in 2 w/v% chitosan solution and their nanocomposites. The combined addition of glycerol and dilution of the chitosan solution is detrimental for the WVP values, which are up to five times higher compared to those of CS_2 based nanocomposites. The addition of NaMMT results in a pronounced reduction of the WVP values (up to 60% for CS/MMT_2 nanocomposite film and up to 25% for CS/MMT_1 nanocomposite film in comparison to CS film). Improvement of barrier properties of polymers by the clay platelets it is known (Lavorgna et al., 2010; Oguzlu & Tihminlioglu, 2010; Rhim et al., 2006) and explained by the creation of a tortuous path for the molecule diffusion. On the other hand the significant increment of WVP with glycerol addition has been previously reported (Lavorgna et al., 2010; Ziani et al., 2008). Glycerol is a relatively small hydrophilic molecule, which can be inserted between adjacent polymeric chains, decreasing intermolecular attractions, thus, facilitating the migration of water vapor molecules (Ziani et al., 2008).

## 4. Conclusions

In the current study the effect of dilution of initial chitosan acetate solution and of the use of a reflux-solution method on the morphology, the mechanical and water barrier properties of chitosan based nanocomposites has been investigated. Based on the obtained results it can be concluded that the reflux-solution method for the performance of the obtained nanocomposites, while dilution of the initial chitosan acetate solution from 2 w/v% to 1 w/v% resulted in inferior performance. More specifically:

(i) Reflux-solution preparation method effect: reflux treatment led to a significant decrease of the chitosan's hydrated crystallinity, a pronounced increase of the stiffness and strength and a considerable reduction of the elongation at break and water vapor permeability (WVP) of the nanocomposite films.
(ii) Dilution of initial chitosan acetate solution from 2 w/v% to 1 w/v% effect: dilution enhanced the chitosan's hydrated crystallinity. Higher crystallinity and less charged amine groups caused by the lower pH values led to a reduction of the stiffness and strength and an increment in the elongation at break. In addition films prepared from diluted chitosan solution absorbed lower amounts of water and showed increased water vapor permeability values.
(iii) Effect of NaMMT addition: addition of NaMMT produced intercalated or partially exfoliated nanocomposites. Addition of NaMMT resulted in enhancement of stiffness (up to 100%) and strength (up to 70%) and dramatic decrease in elongation at break (up to 75%). Both water sorption and water vapor permeability decreased due to the presence of dispersed NaMMT nanoparticles.
(iv) Effect of addition of both glycerol and NaMMT: The incorporation of glycerol favored the opening of the NaMMT clay galleries resulting in intercalated nanocomposite structure. Addition of glycerol resulted in stiffness and strength reduction and increment of elongation/strain at break due to a plasticization effect. Finally undiluted chitosan/glycerol/NaMMT obtained nanocomposites presented mediate values of water permeability between the higher values of the respective diluted films and lower values of chitosan/NaMMT films.

## References

Bangyekan, C., Aht-Ong, D., & Srikulkit, K. (2006). Preparation and properties evaluation of chitosan-coated cassava starch films. *Carbohydrate Polymers*, *63*, 61–71.
Cuq, B., Gontard, N., & Guilbert, S. (1998). Proteins as agricultural polymers for packaging production. *Cereal Chemistry*, *75*(1), 1–9.
Darder, M., Colilla, M., & Ruiz-Hitzky, E. (2003). Biopolymer–clay nanocomposites based on chitosan intercalated in montmorillonite. *Chemistry of Materials*, *15*, 3774–3780.
Epure, V., Griffon, M., Pollet, E., & Avérous, L. (2011). Structure and properties of glycerol-plasticized chitosan obtained by mechanical kneading. *Carbohydrate Polymers*, *83*, 947–952.
Gartner, C., Lopez, B.-L., Sierra, L., Graf, R., Spiess, H. W., & Gaborieau, M. (2011). Interplay between structure and dynamics in chitosan films investigated with solid-state NMR, dynamic mechanical analysis and X-ray diffraction. *Biomacromolecules*, *12*, 1380–1386.
Giannakas, A., Spanos, C. G., Kourkoumelis, N., Vaimakis, T., & Ladavos, A. (2008). Preparation, characterization and water barrier properties of PS/organo-montmorillonite nanocomposites. *European Polymer Journal*, *44*(12), 3915–3921.
Günister, E., Pestreli, D., Unlu, C. H., Atici, O., & Gungor, N. (2007). Synthesis and characterization of chitosan-MMT biocomposite systems. *Carbohydrate Polymers*, *67*, 358–365.
Han, J. H., & Gennadios, A. (2005). Edible films and coatings: A review. In J. H. Han (Ed.), *Innovations in food packaging* (pp. 239–259). San Diego, CA: Elsevier Academic Press.
Hong, S. I., Lee, J. H., Bae, H. J., Koo, S. Y., Lee, H. S., Choi, J. H., et al. (2011). Effect of shear rate on structural, mechanical, and barrier properties of chitosan/montmorillonite nanocomposite film. *Journal of Applied Polymer Science*, *119*, 2742–2749.
Jason, B., Marroquin Rhee, K. Y., & Park, S. J. (2013). Chitosan nanocomposite films: Enhanced electrical conductivity, thermal stability, and mechanical properties. *Carbohydrate Polymers*, *92*(2), 1783–1791.

Jaworska, M., Sakurai, K., Gaudon, P., & Guibal, E. (2003). Influence of chitosan characteristics on polymer properties. I: Crystallographic properties. *Polymer International*, *2*, 198–205.

Kittur, F. S., Kumar, A. B. V., & Tharanathan, R. N. (2003). Low molecular weight chitosans-preparation by depolymerization with *Aspergillus niger* pectinase, and characterization. *Carbohydrate Research*, *338*(12), 1283–1290.

Lavorgna, M., Attianese, I., Buonocore, G. G., Conte, A., Del Nobile, M. A., Tescione, F., et al. (2014). MMT-supported Ag nanoparticles for chitosan nanocomposites: Structural properties and antibacterial activity. *Carbohydrate Polymers*, *102*(15), 385–392.

Lavorgna, M., Piscitelli, F., Mangiacapra, P., & Buonocore, G. G. (2010). Study of the combined effect of both clay and glycerol plasticizer on the properties of chitosan films. *Carbohydrate Polymers*, *82*, 291–298.

Muzzarelli, R. A. A., & Muzzarelli, C. (2002). Natural and artificial chitosan-inorganic composites. *Journal of Inorganic Biochemistry*, *92*, 89–94.

Muzzarelli, R. A. A. (2011). Chitosan composites with inorganics, morphogenetic proteins and stem cells, for bone regeneration. *Carbohydrate Polymers*, *83*, 1433–1445.

Muzzarelli, R. A. A. (2012). Nanochitins and nanochitosans, paving the way to eco-friendly and energy-saving exploitation of marine resources. *Polymer Science: A Comprehensive Reference*, *10*, 153–164.

Muzzarelli, R. A. A., Boudrant, J., Meyer, D., Manno, N., DeMarchis, M., & Paoletti, M. G. (2012). A tribute to Henri Braconnot, precursor of the carbohydrate polymers science, on the chitin bicentennial. *Carbohydrate Polymers*, *87*, 995–1012.

Oguzlu, H., & Tihminlioglu, F. (2010). Preparation and barrier properties of chitosan-layered silicate nanocomposite films. *Macromolecular Symposium*, *298*, 91–98.

Petrova, V. A., Nud'ga, L. A., Bochek, A. M., Yudin, V. E., Gofman, I. V., Elokhovskii, V., et al. (2012). Specific features of chitosan–montmorillonite interaction in an aqueous acid solution and properties of related composite films. *Polymer Science Series A*, *54*(3), 224–230.

Potarniche, C. G., Vuluga, Z., Donescu, D., Christiansen, J. de C., Eugeniu, V., Radovici, C., et al. (2012). Morphology study of layered silicate/chitosan nanohybrids. *Surface and Interface Analysis*, *44*, 200–207.

Rhim, J.-W., Hong, S.-I., Park, H.-M., & Ng, P. K. W. (2006). Preparation and characterization of chitosan-based nanocomposite films with antimicrobial activity. *Journal of Agricultural and Food Chemistry*, *54*, 5814–5822.

Rhim, J.-W., & Ng, P. K. W. (2007). Natural biopolymer-based nanocomposite films for packaging applications. *Critical Reviews in Food Science and Nutrition*, *47*, 411–433.

Suyatma, N. E., Tighzert, L., Copinet, A., & Coma, V. (2005). Effects of hydrophilic plasticizers on mechanical, thermal, and surface properties of chitosan films. *Journal of Agricultural and Food Chemistry*, *53*(10), 3950–3957.

Tang, C., Chen, N., Zhang, Q., Wang, K., Fu, Q., & Zhang, X. (2009). Preparation and properties of chitosan nanocomposites with nanofillers of different dimensions. *Polymer Degradation and Stability*, *94*, 124–131.

Thakhiew, W., Devahastin, S., & Soponronnarit, S. (2010). Effects of drying methods and plasticizer concentration on some physical and mechanical properties of edible chitosan films. *Journal of Food Engineering*, *99*, 216–224.

Wang, S. F., Shen, L., Tong, Y. J., Chen, L., Phang, I. Y., Lim, P. Q., et al. (2005). Biopolymer chitosan/montmorillonite nanocomposites: Preparation and characterization. *Polymer Degradation and Stability*, *90*, 123–131.

Wang, X., Du, Y., Yang, J., Tang, Y., & Luo, J. (2006). Preparation, characterization and antimicrobial activity of chitosan/layered silicate nanocomposites. *Polymer*, *47*, 6738–6744.

Xie, D. F., Martino, V. P., Sangwan, P., Way, C., Cash, G. A., Pollet, E., et al. (2013). Elaboration and properties of plasticised chitosan-based exfoliated nano-biocomposites. *Polymer*, *54*(14), 3654–3662.

Xu, Y., Ren, X., & Hanna, M. A. (2006). Chitosan/clay nanocomposite film preparation and characterization. *Journal Applied Polymer Science*, *99*, 1684–1691.

Ziani, K., Oses, J., Coma, V., & Mate, J. I. (2008). Effect of the presence of glycerol and Tween 20 on the chemical and physical properties of films based on chitosan with different degree of deacetylation. *LWT – Food Science and Technology*, *41*, 2159–2165.